



## A numerical simulation to achieve a high efficiency: Influence and optimization of thickness and doping concentration of emitter layer of heterojunction solar cells

\*Naceur SELMANE<sup>1</sup>, Ali CHEKNANE<sup>1</sup>, Hikmat S. HILAL<sup>2</sup>

<sup>1</sup>Electronic department. Laghouat university, Semiconductors and Functional Materials Laboratory, LSMF, A- 03000 Laghouat, Algeria (naceur\_af@yahoo.fr)

<sup>2</sup>Department of Chemistry (SSERL laboratory) / An-Najah National University, Nablus, Palestine

### Article history

Received: 2019-12-25

Accepted: 2020-07-11

### Abstract

HIT silicon hetero-junction TCO/n-a-Si:H/i-a-Si:H/p-c-Si/p<sup>+</sup>-a-Si:H/BSF solar cells attract special interest due to their suitability and high efficiencies, in this study, we present a numerical simulation of the influence of emitter layer on the performance of silicon proposed heterojunction solar cells. The basic parameters of heterojunction solar cells, such as layer thickness, doping concentration, interface defect density, back surface field (BSF) layer, are important factors that influence the carrier transport properties and the performance of the solar cells.. Thickness and doping concentration of the emitter layer are optimized here. With optimal parameters, high simulated solar cell characteristics can be achieved in terms of conversion efficiency ( $\eta=25.62\%$ ), open circuit potential ( $V_{OC}= 744$  mV), short circuit current density ( $J_{SC}= 42.43$  mA/cm<sup>2</sup>) and fill factor (FF=83.7%). *The Automat for Simulation of Heterostructures (AFORS-HET)* program is used.

**Key-words:** *AFors-HET; Heterojunction solar cells; Emitter layer; Doping concentration.*

### Résumé

Les cellules solaires à hétéro-jonction à base de silicium : TCO / n-a-Si: H / ia-Si: H / p-c-Si / p<sup>+</sup> -a-Si: H / BSF attirent un intérêt particulier en raison de leur adéquation et de leur efficacité élevée, dans cette étude, nous présentons une simulation numérique de l'influence de la couche d'émetteur sur les performances des cellules solaires à hétérojonction à base de silicium proposées. Les paramètres de base des cellules solaires à hétérojonction tels que l'épaisseur de couche, la concentration de dopage, la densité des défauts d'interface, le champ de surface arrière (BSF), sont des facteurs importants qui influencent sur les propriétés de transport des porteurs de charges et les performances des cellules solaires. L'épaisseur et la concentration de dopage de la couche émettrice y sont optimisées. Avec des paramètres optimaux, les caractéristiques des cellules solaires simulées peuvent être obtenues en termes d'efficacité de conversion ( $\eta=25,62\%$ ), tension en circuit ouvert ( $V_{CO}=744$  mV), densité de courant de court-circuit ( $J_{cc}=42,43$  mA / cm<sup>2</sup>) et facteur de forme (FF= 83,7%). Le programme *Automat for Simulation of Heterostructures (AFORS-HET)* est utilisé.

**Mots-clés :** *Afors-HET; Cellules solaires à hétérojonction; Couche d'émetteur; Concentration de dopage;*

\* Corresponding author. Tel./fax: +213 662698464.

E-mail address: naceur\_af@yahoo.fr.

## 1. Introduction

Solar cells based on thin film silicon/crystalline silicon hetero-junctions attract interest. They combine advantages of high stability, high conversion efficiency of c-Si[1], ambient temperature, low cost, ease to control thickness and doping of thin silicon film. The a-Si:H/c-Si hetero-junctions were first studied in early 1980s[2]. Twenty years later, Sanyo invented HIT solar cell using plasma enhanced chemical vapour deposition (PECVD) deposited onto n-type CZ wafer. The new cell showed high conversion efficiency (20.7%) when using multi layers. Intrinsic buffer layer, back side face (BSF) layer and TCO transparent conductor oxide all resulted in improved properties for the hetero-junction solar cell [3]. Other parameters involved in HIT solar cells, such as thickness, doping concentration, different re-combinations (Radiative, Auger, SRH) at interface due to surface states and defects distribution type [4-6] also affect solar cell performance. Cell performance depends on quality and type of the thin film silicon material used and on optimisation of device design, such as layer properties (thickness, doping) and numbers. The quality of interfaces between the different layers is another important factor. Amorphous emitter layer, and their concentrations doping, and thickness, should also be considered.

The thickness and doping concentration of emitter layer are also important parameters to improve solar cell performance [7-9].

By numerical simulation, a prospective TCO/n-a-Si:H/i-a-Si:H/p-c-Si/p+a-Si:H BSF solar cell is proposed here with high performance. Photovoltaic characteristics such as the conversion efficiency ( $\eta$ ), fill factor (FF), open-circuit potential ( $V_{OC}$ ) and the short circuit current density ( $J_{SC}$ ), have all been assessed. Simulation helps exploration of solar cells with special characteristics and low cost, and facilitates the understanding of different phenomena that occur in heterojunction solar cells. Automat for Simulation of Heterostructures (AFORS-HET) software is used to optimize parameters, such as thickness, doping concentration and work function to obtain high performance solar cells[3,7,10-15]. This work is focused on effects on the emitter layer (n-a-Si) doping concentration. The effects of such parameters on performance of TCO/n -a-Si:H/i-a-Si:H/p- c-Si/p+ a-Si:H BSF solar cells are investigated.

In recent reports, simulation study showed that extremely low thicknesses and high doping concentrations may yield higher performance Si:H solar cells[3,5,6]. Energy band structure, quantum efficiency, current density and generation/recombination phenomena were analyzed to achieve higher performance. In the present study, a closer look at the influence of emitter layer thicknesses, on the performance of the proposed solar cell, is described. Parameter optimizations will also be described. Conversion efficiency 25.62%,  $V_{OC}$  744 mV,  $J_{SC}$  42.43 mA/cm<sup>2</sup> and FF 83.7%, can be obtained through simulation for TCO/n-a-Si:H/i-a-Si:H/p- c-Si/p+a-Si:H/BSF solar cells.

## 2. Methods and simulation details:

AFORS-HET, based on solving the one-dimensional Poisson and the continuity equations using Shockley–Read–Hall recombination statistics, is widely used for studying heterojunction solar cells[3, 7, 10-12]. The simulated HIT solar cells have the structure ZnO/ a-Si:H/n a-Si:H/i-c-Si/p /Al BSF /Al, where the absorber layer is pc-Si, n a-si is the emitter layer, i a-Si it is the passivation layer of intrinsic type, TCO is the transparent conductive oxide (ZnO in this study). Figure 1 schematically describes the solar cell used here. In the present simulation, AM 1.5 radiation was used as the illumination source with a power density of 100 mW/cm<sup>2</sup>. For the p-c-Si substrate, oxygen defects with a density of  $1 \times 10^{11} \text{ cm}^{-3} \text{ eV}^{-1}$  located at 0.55 eV above EV (EV + 0.55) are assumed. The defect states involve a single distribution for electrons ( $1 \times 10^{-14}$ ) and holes ( $1 \times 10^{-14}$ ).

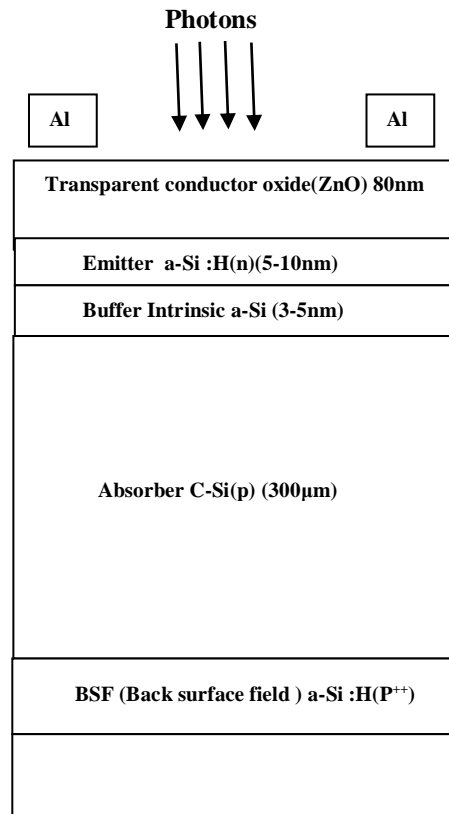


**Figure 1.** Schematic diagram of a n-a-Si:H/i-a-Si:H/p-c-Si/p+a-Si:H/BSF solar cell.

The defect density (Dif) at the i-a-Si:H/c-Si interface is  $1 \times 10^9 - 1 \times 10^{13} \text{cm}^{-2} \cdot \text{eV}^{-1}$  with continuous distribution [13]. The main simulated parameters of the different layers are listed in Table 1 [7, 14-16]. The surface recombination rates of electrons and holes are both set as  $1 \times 10^7 \text{cm/s}$ . The ZnO layer is used as a TCO. The light reflection of front contact is set to be at the extreme standard values for such devices (0.1 and 1.0). The AFORS-HIT software environment, which is one dimensional solar cell device simulator, is employed here. The important characteristics to be extracted are  $V_{OC}$ , JSC, and  $\eta$ . The integration of the ZnO layer in the heterojunction cell clearly affects its performance.

**Table 1:** Main simulation parameters used for different layers in the hetero-junction solar cell

	a-Si H(n)	a-Si H(i)	c-Si H(p)	Al-BSF (P <sup>+</sup> )
Layer thickness (nm)	10	5	$3 \times 10^5$	$5 \times 10^3$
Dielectric constant (dk)	11.9	11.9	11.9	11.9
Band gap Eg(eV)	1.74	1.72	1.12	1.72
Electron affinity(eV)	3.9	3.9	4.05	4.05
Effective conduction band density( $\text{cm}^{-3}$ )	$1 \times 10^{20}$	$1 \times 10^2$	$2.8 \times 10^{19}$	$2.8 \times 10^{19}$
Effective valence band density( $\text{cm}^{-3}$ )	$5 \times 10^{18}$	$1 \times 10^2$	$1.04 \times 10^{19}$	$1.04 \times 10^{19}$
Electron mobility( $\text{cm}^2 \text{V}^{-1} \text{s}^{-1}$ )	20	20	1040	20
Hole mobility( $\text{cm}^2 \text{V}^{-1} \text{s}^{-1}$ )	5	5	412	5
Doping concentration of donors ( $\text{cm}^{-3}$ )	$1 \times 10^{20}$	0	0	0
Doping concentration of acceptors ( $\text{cm}^{-3}$ )	0	0	$1.5 \times 10^{19}$	$1 \times 10^{20}$
Thermal velocity of electron ( $\text{cm}^{-3} \text{s}^{-3}$ )	$1 \times 10^7$	$1 \times 10^7$	$1 \times 10^7$	$1 \times 10^7$
Thermal velocity of holes ( $\text{cm}^{-3} \text{s}^{-3}$ )	$1 \times 10^7$	$1 \times 10^7$	$1 \times 10^7$	$1 \times 10^7$
Auger recombination coefficient for electrons( $\text{cm}^6 \text{s}^{-1}$ )	0	0	$2.2 \times 10^{-31}$	$2.2 \times 10^{-31}$
Auger recombination coefficient for holes ( $\text{cm}^6 \text{s}^{-1}$ )	0	0	$9.9 \times 10^{-32}$	$9.9 \times 10^{-32}$

### 3. Results and discussion

#### 3.1. The role of i-a-Si:H (buffer layer) and p<sup>+</sup>-a-Si:H (BSF layer)

The performance of a given solar cell is influenced by addition of each layer. The integration of i-a-Si:H buffer layer and BSF layer was thus investigated here. Photo-current density vs. applied potential(J-V) characteristics are shown in Figure 2. The J-V plots change by insertion of i-a-Si:H layer and BSF layer, as compared to the reference a-n -Si/c-p-Si solar cell. The efficiency changes from 13.5% (with no buffer layer) to 17.78% with the intrinsic layer. When the BSF layer is included, the efficiency increases to more than 20%. It is well known that a high quality i-a-Si:H buffer layer acts as the passivation for the a-Si:H/c-Si interface in HIT solar cells. The middle band diagram in Figure 3 shows that the i-a-Si:H buffer layer can hinder the photon-generated carrier recombination from the n-a-Si:H emitter layer to the p-c-Si base layer. Thus the short-circuit current density of the solar cell is improved by inserting an i-a-Si:H buffer layer. Moreover, the absorber (band gap  $E_g=1.12\text{eV}$ ) is connected to i-a-Si:H buffer ( $E_g=1.72\text{eV}$ ) which is in turn connected with the emitter layer n-a-Si that forms contact for electrons (band gap  $E_{g1}=1.74\text{eV}$ ) and another contact in the other side for holes with a band gap  $E_{g2}=1.72\text{eV}$ . So the p-c-Si absorber layer has a band gap different from the gaps of the two hetero-interfaces  $E_{g1}=1.74\text{eV}$  for the emitter layer and  $E_{g2}=1.72\text{eV}$  for i-a-Si:H buffer layer. On the left hand side of the structure, generated mobile electrons are collected in the n-a-Si layer whereas the holes are reflected. On the right hand side of the structure, the mobile holes are collected in the p<sup>+</sup>-a-Si:H BSF-contact whereas the electrons are reflected,

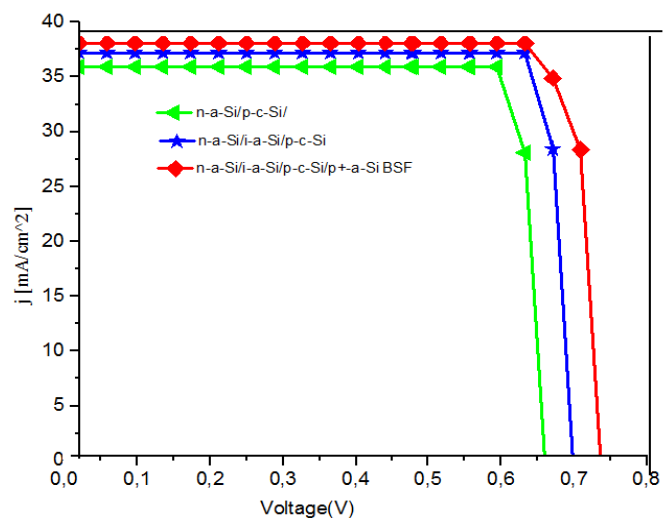


**Figure 2:** J-V plots for the HIT solar cell with and without i-a-Si:H buffer and p<sup>+</sup>-a-Si:H BSF layers.

Figure 3 shows the band diagram of an a-Si:H/c-Si solar cell after integration of the i-a-Si:H buffer layer or p+-a-Si:H BSF layer. The band discontinuities  $\Delta E_c$  for the conduction band and  $\Delta E_v$  for the valence band (quantum deep) at both interfaces are caused by the different band gap of c-Si. The front n-a-Si:H/p-c-Si contact is similar to a p-n homo-junction. It also forms a selective n-contact because the band offset in the valence band hinders holes from entering into the a-Si:H emitter. The p+-a-Si:H back contact forms a BSF, where the electric field forces the electrons away from the interface and attracts the holes. Moreover, the band offset in the conduction band  $\Delta E_c$  hinders the electrons from diffusing into the p+ a-Si:H layer, which leads to limit the  $V_{oc}$  from the back contact compared to those without BSF layer. To improve the performance of the present solar cell, TCO (ZnO) was integrated. With a wide band gap (~3.4eV) ZnO increases the probability of absorption of the photons with different wavelengths, and decreases the number of reflected photons. The p-c-Si layer will thus absorb more incident photons, yielding more electron-hole pair formation. The  $J_{sc}$  will thus increase. Other characteristics, FF,  $V_{oc}$ ,  $J_{sc}$  and  $\eta$  will also be enhanced with the insertion of the ZnO layer.

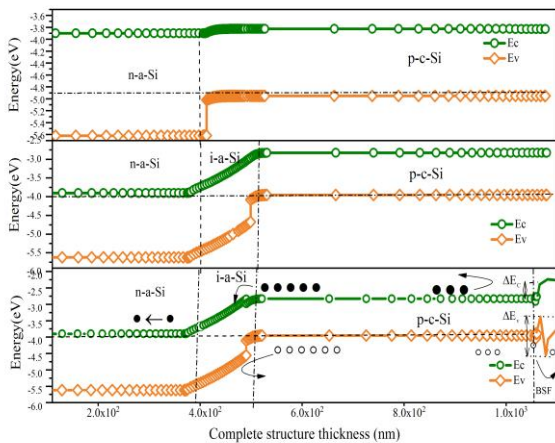


Figure 3: The corresponding band diagram for the HIT solar cell with and without i-a-Si:H buffer and p+-a-Si:H BSF layers

**Table 2:** Performance of HIT solar cell with and without i-a-Si:H buffer and p+-a-Si:H BSF layers.

Solar cell	$J_{sc}$ (mA/cm <sup>2</sup> )	$V_{oc}$ (mV)	FF	$\eta\%$
n-a-Si/p-c-Si	36.14	663.7	72	13.5
n-a-Si/i-a-Si/p-c-Si	37.65	699.4	74.24	16.78
n-a-Si/i-a-Si/p-c-Si/P+-a-Si BSF	38.23	738.2	78	19.42

### 3.2. The influence of thickness emitter layer

The performance of the solar cell is influenced by the variation of the thickness of each layer in the hetero-junction. In this work, we interest by the Al-doped ZnO(TCO) and emitter layer thicknesses, The Figure 4(a,b) shows that when the thickness of the emitter layer varies from 5 to 15 nm, the values of FF,  $V_{oc}$ ,  $J_{sc}$  and  $\eta$  change. Maximum efficiency of 24% can be observed for 5nm thickness. Value of FF slightly increases by increasing the layer thickness from 5 to 15 nm, while values of  $J_{sc}$  and  $V_{oc}$  steadily decrease. The  $V_{oc}$  can be simply expressed as .

$$V_{oc} = \frac{KT}{q} \ln \left( \frac{j_{sc}}{j_0} + 1 \right) \quad (1)$$

So, leakage current ( $j_0$ ) in the cell lowers  $V_{oc}$  [17].  $V_{oc}$  does not directly depend on thickness of the n-type emitter [18] in the thickness range 5-15 nm, since the thickness 6nm exhibits maximum  $V_{oc}$  value. Based on Figure 4,  $J_{sc}$  increases with lower emitter layer thickness. This is due to lowered recombination rate as discussed above. Over all, the 5nm thickness shows optimal value for cell performance taking into consideration values of FF,  $V_{oc}$ ,  $J_{sc}$  and  $\eta$  together. With higher thickness, the generated carriers recombine before reaching the Ohmic contacts (electrodes) at the surface. Excessive minority carriers are prone to undergo the unwanted recombination. This is because the higher thickness increases the probability that the carriers recombine in the emitter layer before reaching the surface. Moreover, the diffusion length is related to the lifetime, which is defined as “the average time between the creation of the carrier and its recombination in a material, without electrical contact”. Life time is related to diffusion length (L) by:  $L = \sqrt{D\tau}$ . Smaller thickness of n-a-Si emitter increases the lifetime of hole and electron minority carriers. Longer lifetimes are desirable to give electron-hole pairs higher chance to reach the surface, and to yield higher photo-current. Moreover, the emitter layer helps create the p-n junction effect, within the charge separating region, essential to produce photo-current in solar cells. Therefore, the n-a-Si:H emitter layer should be as thin as possible to inhibit recombination, and to allow absorbed photons to pass to the c-p-Si absorber layer. Most electrons are thus generated in the absorber layer, which leads to higher solar cell performance.

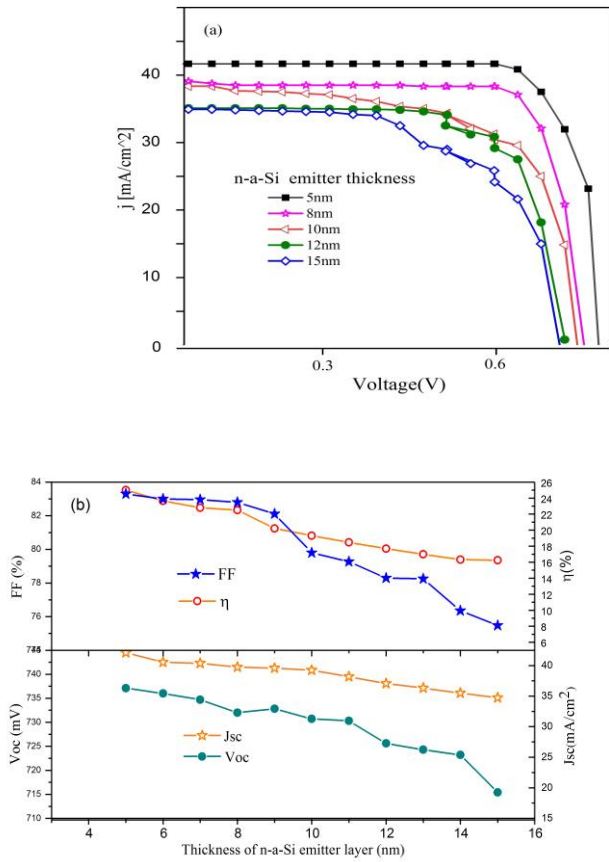


**Figure 4:** Effect of n-a-Si:H emitter thickness on a)  $j(v)$  plots HIT solar cell b) on HIT solar cell characteristics  $V_{OC}$ ,  $J_{SC}$ , FF and  $\eta$

### 3.3. Effect of emitter layer doping density

The n-a-Si emitter layer doping density may affect the performance of the solar cell. Figure 5 (a,b) shows that as doping concentrations decreases below  $(2 \times 10^{19} \text{ cm}^{-3})$ , the  $V_{OC}$  value sharply decreases. The  $J_{SC}$  also decreases when decreasing doping concentration below  $2 \times 10^{19} \text{ cm}^{-3}$ . At lower doping concentrations, the electric field leads to accumulation of electron and hole carriers at the band offset of the valence and conduction band interface. These results from the different band gap values of the materials involved in the hetero-junctions. Recombinations (Radiative, Auger and SRH) are encouraged along the n-a-Si emitter and the depletion region which affects efficiency.

Figure 5 (a,b) shows that with higher doping concentrations  $(> 2 \times 10^{19} \text{ cm}^{-3})$  in the n-a-Si layer, both  $V_{OC}$  and  $J_{SC}$  values increase. The depletion region builds up a higher barrier with higher electric field that facilitates minority carrier (electrons) diffusion from the c-p-Si absorber layer to n-a-Si and to reach the front contact. Same thing occurs for the holes in the other side. This minority carrier diffusion results from the direction of electric field build-up caused by positive charges created in the n-a-Si and negative charges

created in the c-p-Si absorber layer. The electric field favours the displacement of the electrons while moving in the direction opposite to it. Same logic applies to the hole motions.

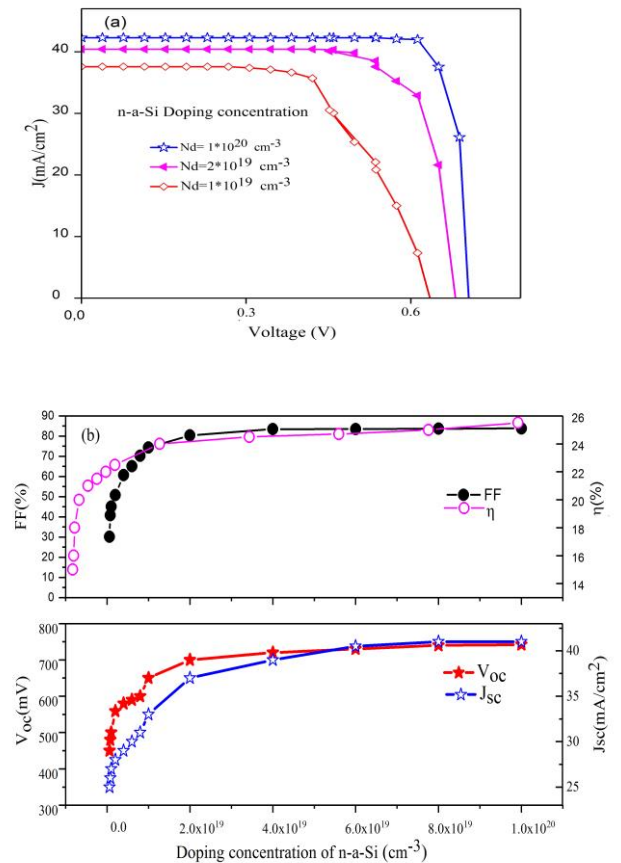


**Figure 5:** Effect of n-a-Si:H layer doping concentration on a)  $j(v)$  plots HIT solar cell b) on HIT solar cell parameters  $V_{OC}$ ,  $J_{SC}$ , FF and  $\eta$ .

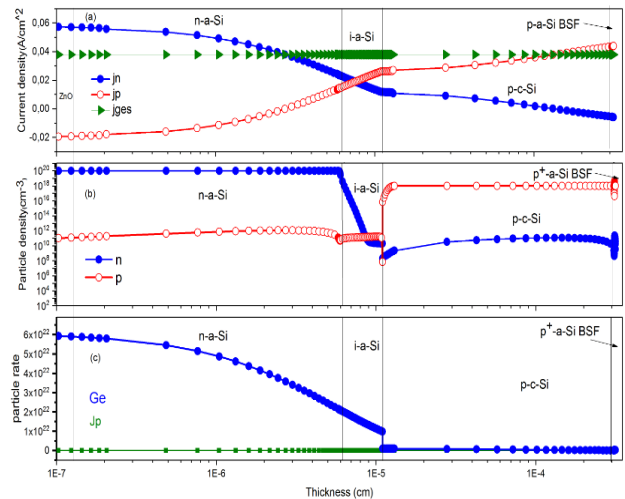
Therefore, in a weak electric field, charge accumulation occurs leading to increased recombinations. In case of strong electric field, recombination rate is lowered as holes are driven away from the interface. Electrons, that reach the space charge region, are accelerated by this electric field towards the front contact. Figure5 (a,b) shows that at doping density  $2 \times 10^{19} \text{ cm}^{-3}$  or higher, in the n-a-Si emitter layer, the  $J_{SC}$  reaches higher than  $43 \text{ mA/cm}^2$ ,  $\eta$  reaches  $\sim 25.54\%$ , and FF slightly increases from  $78.5\%$  to  $83.5\%$ . The results are in congruence with earlier reports [3].

In the absorber layer, the majority carriers are the holes and the minority carriers are the electrons, while in the emitter layer the electrons are the majority carriers and the holes electrons are the minority carriers. Fig.6 a shows the simulated current density vs. distance across the four layers, n-a-Si/i-a-Si/p-c-Si/P<sup>+</sup>-a-Si BSF. In the n-a-Si emitter the current density is n-type (electrons are majority charges

carriers). In the c-p-Si holes are also majority carriers as the current in the junction due to the minority electrons results by electric field. The absorber layer exhibits p-type (holes are majority carriers). The total current density involves both n and p-type carriers as:  $J=J_n+J_p$  where each has two components (drift and diffusion). Fig.6 b shows the charge carrier concentration in each layer. The electron carrier concentration in the n-a-Si layer is estimated to be  $10^{20} \text{cm}^{-3}$ , and the minority carrier (hole) density is estimated to be  $10^{10} \text{cm}^{-3}$ . In the a-i-Si buffer, the electron density concentration varies from  $10^{20}$  to  $10^7 \text{cm}^{-3}$ , and the hole concentration varies from  $10^{18}$  to  $10^{12} \text{cm}^{-3}$  [13]. In the c-p-Si absorber layer the concentration of the majority carriers (holes) is  $10^{18} \text{cm}^{-3}$ , and the electron minority concentration is  $\sim 10^{11} \text{cm}^{-3}$ . The current density is also distributed along the interfaces. In the BSF layer the holes accumulate at the contact with c-p-Si absorber due to the valence band offset. This creates deep potential and discontinuity in the conduction bands leading to Shockley-Read-Hall recombination (SRH). In SRH, also called trap-assisted recombination, the electron in transition between bands passes through a new energy state (localized state) created within the band gap by a dopant or by a defect in the crystal. Such energy states behave as traps. Non-radiative recombination occurs primarily at such sites. The energy is exchanged in the form of lattice vibrations (phonons).

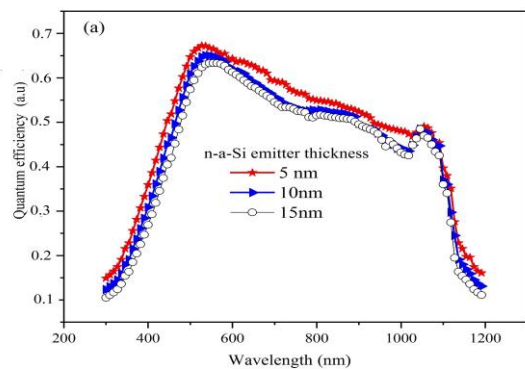
Since traps can absorb differences in momentum between the carriers, SRH is the dominant recombination process in silicon and other indirect bandgap materials. However, trap-assisted recombination may also dominate in direct bandgap materials under conditions of very low carrier densities or in materials with high density of traps such as Perovskites.

Understanding the transport phenomena clarifies the electric properties of simulated solar cells. Recombination and generation phenomena shown in Fig. 6 c help understand these properties. Generation of electron-hole pairs in the n-a-Si emitter layer caused by high photon flux absorbed by TCO, occurs at high particle rate ( $\sim 5 \times 10^{22} \text{cm}^{-3}/\text{s}$ ), (Fig.6 c), while the recombination is almost negligible. This is assisted by the high doping density and the low thickness of n-a-Si emitter layer. Electric field build-up occurs and drives positively charged holes away from the interface. On the other hand, space charge region electrons are driven by the electric field towards the front contact with no recombination losses.



**Figure 6.** Some electrical properties changes with distance across the HIT solar cell showing: a) Current density, b) Charge carrier concentration and c) Generation and recombination.

Quantum Efficiency (QE) measurement explores the performance of a solar cell at different incident wavelengths. With ZnO front contact the cell exhibits higher response in near UV-Visible and near IR(400-1100nm) than the cell without ZnO layer, but there is lowering in QE response caused by the low diffusion length compared with ideal response. The forms of the spectra at wave lengths shorter than 400nm and longer than 1100 nm are due to the rear surface and other recombinations that happen at the front and back contacts. At 1100nm wavelength, no absorption occurs below the band gap, and the QE becomes zero at longer wave lengths. Figure 7 indicates that the optimal doping density for the emitter is  $2 \times 10^{19} \text{cm}^{-3}$  or higher, the optimal thickness is 5 nm and the optimal concentration is  $2 \times 10^{19} \text{cm}^{-3}$ .





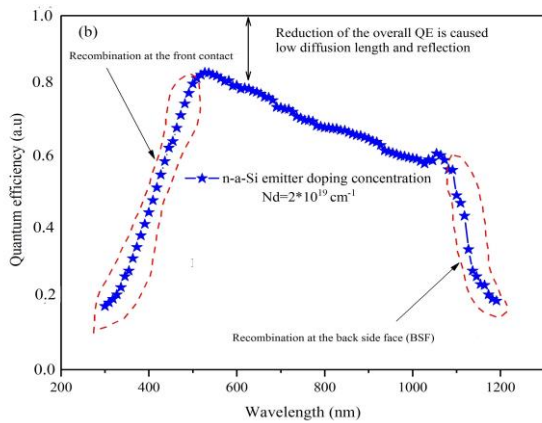


**Figure 7.** Simulated QE characteristics for the HIT solar cell vs. incident radiation wavelength, for n-a-Si emitter layer a) with different thicknesses and b) with  $N_d=2 \times 10^{19} \text{ cm}^{-3}$  or higher doping concentration

Therefore, the performance of hetero-junction cell depends on TCO front contact, and the on n-a-Si emitter layer. QE measurement further confirms the possibility to improve the performance of HIT solar cells by adding a ZnO layer in the simulated structure. Figure 8 shows the optimized simulated J-V characteristics, with  $\eta$  (25.62%),  $V_{OC}$  (744 mV),  $J_{SC}$  (42.43 mA/cm<sup>2</sup>) and FF (83.7%). Therefore, Solar cell performance can be optimized by better understanding of carrier transport mechanism at the interface. The optimized parameters are summarized in table 3.

**Table 3.** The optimized parameters for HIT solar cell

Layer	Thickness(nm)	Doping concentration (cm <sup>-3</sup> )
Emitter layer	5	$>2 \times 10^{19}$

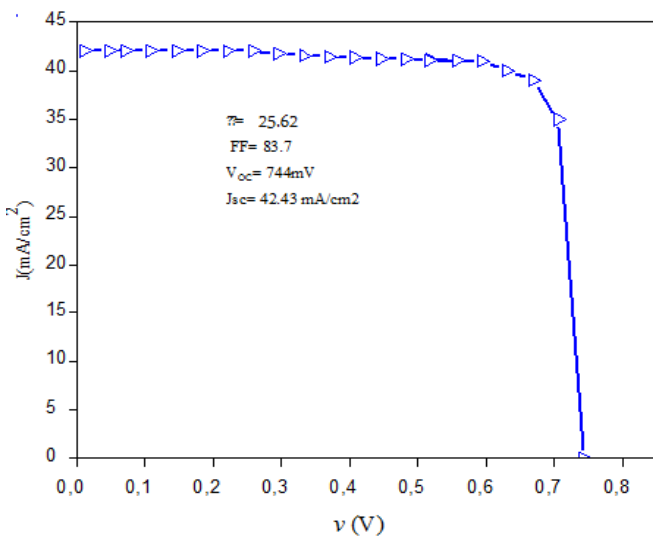


**Figure 8.** A simulated J-V plot for the HIT solar cell with optimized characteristics.

#### 4. Conclusion

High performance hetero-junction a-Si:H/c-Si solar cells can be constructed. Band discontinuities and different layer parameters (emitter layer) affect solar cell performance as confirmed here using AFORS-HET simulation program. Thickness and doping density of the n-a-Si emitter layer, as well affect HIT solar cell characteristics, and can be optimized. The effect of adding a-i-Si buffer and P<sup>+</sup>-a-Si back side face (BSF) layers is studied. Such addition enhances the solar cell performance. Lower n-a-Si:H emitter layer thickness (~5nm) and higher doping density ( $2 \times 10^{19} \text{ cm}^{-3}$  or higher) enhance the HIT solar cell performance. With optimal conditions, high solar cell characteristics ( $\eta = 25.62\%$ ,  $V_{OC} = 744 \text{ mV}$ ,  $J_{SC} = 42.43 \text{ mA/cm}^2$ , FF: 83.7%) can be reached for the TCO/n-a-Si:H/i-a-Si:H/p- c-Si/p+a-Si:H/BSF solar cell.

#### Acknowledgment

Authors are grateful to the Amar Telidji University, for providing financial support through the laboratory of semiconductors and functional materials

#### References

- [1]. K.Masuko, M.Shigematsu, Taiki Hashiguchi, D.Fujishima, M.Kai, N.Yoshimura, T.Yamaguchi, Y.Ichihashi, T. Achievement of more than 25% conversion efficiency with crystalline silicon heterojunction solar cell, IEEE Journal of Photovoltaics; 4(2014)1433-1435.
- [2]. A. Goetzberger and V.U. Hoffman, Photovoltaic Solar Energy Generation, N.Y., Springer (2005).
- [3]. L.Jian, H.Shihua, and H.Lü, Simulation of a high-efficiency silicon-based heterojunction solar cell, Journal of Semiconductors, 36(2015) 044010/1-8.
- [4]. M. Izzi, M. Tucci and L. Serenelli, TCO optimization in Si heterojunction solar cells on p-type wafers with n-SiOx emitter, Energy Procedia, 84 (2015) 134–140.
- [5]. L. Zhao, C. L. Zhou, H. L. Li, H. W. Diao, W. J. Wang, Role of the work function of transparent conductive oxide on the performance of amorphous/crystalline silicon heterojunction solar cells studied by computer simulation. Physica Status Solidi A, Applications and Materials Science, (2008) 1215–1221.
- [6]. L. Zhao, C. L. Zhou, H. L. Li, H.W.Diao and W.J.Wang Design optimization of bifacial HIT solar cells on p-type silicon substrates by simulation. Sol Energy Materials and Solar Cells, 92 (2008) 673-681.
- [7]. N. Dwivedi, S. Kumar, A. Bisht, K. Patel and S.Sudhakar, Simulation approach for optimization of device

- structure and thickness of HIT solar cells for to achieve to 27% efficiency. *Solar Energy*, 88, (2013) 31-41.
- [8]. W. Lisheng, C. Fengxiang and A. Yu, Simulation of high efficiency heterojunction solar cells with AFORS-HET. *Journal of Physics: ConferenceSeries*,276 (2011) 012177/1-9.
- [9]. Q. Liu, X.J. Ye, C. Liu C, M-B. Ming, Performance of bifacial HIT solar cells on n-type silicon substrates. *OptoelectronicsLetters*, 6 (2010) 108-111.
- [10]. R.Stangl, A.Froitzheim , M.Kriegel ,T.Brammer, S.Kirste , L.Elstner , H.Stiebig, Afors-HET, A numerical pc-program for simulation of (thin film) heterojunction solar cells, version 2.0 (open-source on demand), to be distributed for public Hahn-Meitner-Institut Berlin (HMI), Abteilung Silizium Photovoltaik, Kekulé-Str. 5, D-12489 Berlin, Germany
- [11]. M. Sharma, S. Kumar, N. Dwivedi, S. Juneja, A.K.Gupta, S. Sudhakar and K. Patel,Optimization of band gap, thickness and carrier concentrations for the development of efficient microcrystalline silicon solar cells:A theoretical approach,*SolarEnergy*,97 (2013) 176–185.
- [12]. A. Morales-Acevedo, N. Hernández-Como and G. Casados-Cruz,Modeling solar cells:a method for improving their efficiency. *Mater Science and Engineering B*, 177 (2012)1430-1435.
- [13]. N. Selmane, A.Cheknane, M. Aillerie, and Hikmat S. Hilal, Effect of ZnO-Based TCO on the Performance of a-Si H(n)/a-Si H(i)/c-Si H(p)/Al BSF(p+)/Al Heterojunction Solar Cells ,*Environmental Progress & Sustainable Energy*,( 2018) ,DOI 10.1002/ep.13114
- [14]. T. Zarede H. Lidjici,M. Fathi . A. Mahrane , Study and Simulation of the Heterojunction Thin Film Solar Cell a-Si(n)/a-Si(i)/c-Si(p)/a-Si(i)/a-Si(p), *Journal of Electronic Materials*, 45(2016), , Issue 8, 3943–3948.
- [15]. M. Izakiand T. Omi, Transparent zinc oxide films prepared by electrochemical reaction, *Applied Physics Letters*, 68 (1996) 2439.
- [16]. A. Boughelout R. Macaluso I. CRUPI B. MEGNA,Improved Cu2O/AZO Heterojunction by Inserting a Thin ZnO Interlayer Grown by Pulsed Laser Deposition *Journal of Electronic Materials*, 48 (2019) 4381-4388.
- [17]. M. Boumaour S. Sali A. Bahfir S. Kermadi, L. Zougar, N. Ouarab, A. Larabi, Numerical Study of TCO/Silicon Solar Cells with Novel Back Surface Field, *Journal of Electronic Materials*, 45 (2016) 3929–3934.
- [18]. N. BOUKORTT, S. PATANÈ, B. HADRI, ELECTRICAL Characterization of n-ZnO/c-Si 2D Heterojunction Solar Cell by Using TCAD Tools, *Silicon*, 10 (2018) 2193-2199.
- [19]. K. Yoshikawa, Hayato Kawasaki, Wataru Yoshida, Toru Irie, Katsunori Konishi, Kunihiko Nakano, Toshihiko Uto, Daisuke Adachi, Masanori Kanematsu, Hisashi Uzu and Kenji Yamamoto, Silicon heterojunction solar cell with interdigitated back contacts for a photoconversion efficiency over 26%, *Nature Energy*,2 (2017), Article number: 17032|
- [20]. X. Wen, X.Zeng, W. Liao, Q. Lei,S. Yin, An approach for improving the carriers transport properties of a-Si:H/c-Si heterojunction solar cells with efficiency of more than 27%. *Solar Energy*, 96 (2013) 168-176.
- [21]. W. Jianqiang, G. Hua, Z. Jian, M. Fanyingand Y. Qinghao, Investigation of an a-Si/c-Siinterface on a c-Si (P) substrate by simulation. *Journal of Semiconductors*,33 (2012) 033001/1-7.
- [22]. S. Zhong, X. Hua, W. Shen, Simulation of high-efficiency crystalline silicon solar cells with homo-hetero junctions.IEEE Explore Digital Library: IEEE Trans Electron Devices, 60 (2013) 2104-2110.
- [23]. N. Jensen, U. Rau, R. M. Hausner, S. Uppal, L. Oberbeck, R. B. Bergmann, and J. H. Werner, Recombination mechanisms in amorphous silicon/crystalline siliconheterojunction solar cells. *Journal of Applied Physics*,87 (2000) 2639-2645.
- [24].M.Tanaka, M.Taguchi, T.Matsuyama, T.Sawada, S.Tsuda, S. Nakano, H.Hanafusa and Y.Kuwano, Development of new a-Si/c-Si heterojunction solar cells: ACJ-HIT (artificially constructed junction-heterojunction with intrinsic thin-layer). *Japanese Journal of Applied Physics*,31 (1992) 3518-3522.